

Supplementary material for EPAPS

Direct observation of Dirac cones and a flatband in a honeycomb lattice for polaritons.

T. Jacqmin,¹ I. Carusotto,² I. Sagnes,¹ M. Abbarchi,^{1,*} D. D. Solnyshkov,³
G. Malpuech,³ E. Galopin,¹ A. Lemaître,¹ J. Bloch,¹ and A. Amo¹

¹Laboratoire de Photonique et Nanostructures, CNRS/LPN, Route de Nozay, 91460 Marcoussis, France

²INO-CNR BEC Center and Dipartimento di Fisica, Università di Trento, I-38123, Povo, Italy

³Institut Pascal, PHOTON-N2, Clermont Université, Université Blaise Pascal,

CNRS, 24 avenue des Landais, 63177 Aubière Cedex, France

(Dated: January 22, 2014)

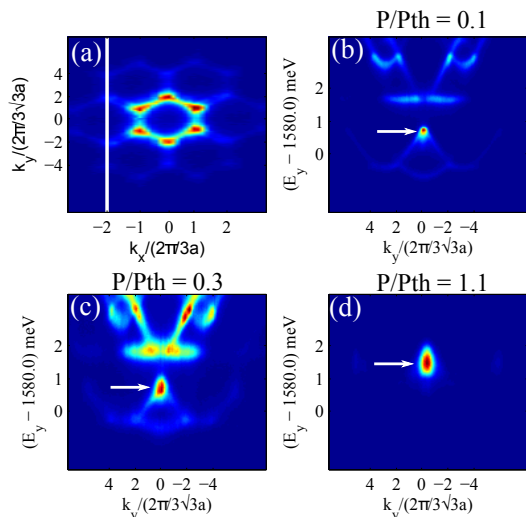


FIG. 1. Photoluminescence emission in the far field: (a) at the Dirac points energy at very low pump intensity, (b) energy dispersion along the white line in (a) at pump power $P/P_{th} = 0.1$, (c) $P/P_{th} = 0.3$ and (d) $P/P_{th} = 1.1$

CONDENSATION IN THE π^* BAND: EXPERIMENTS

In order to prove that the state at which polariton condensation takes place is located at the top of the π^* band, as reported in Fig. 3, we show here a detailed power dependence of the emission across the condensation threshold. At low power (Fig. 1(b)), below threshold, all the low energy bands are populated. At the Γ point a brighter point is observed showing efficient relaxation towards that state. When we approach the threshold for condensation we observe that particles start to accumulate at the top of the π^* band (Fig. 1(c)). Above threshold it is that particular state the one that becomes macroscopically occupied (Fig. 1(d)). Note that the π and π^* bands continuously blueshift when increasing the excitation power due to the repulsive interactions between polaritons populating that band and the highly populated exciton reservoir located at the bare exciton energy (about 20 meV above in energy).

CONDENSATION IN THE π^* BAND: SIMULATIONS

To simulate polariton condensation in the honeycomb structure we have used a 2D Gross-Pitaevskii equation with additional terms describing the polariton lifetime, spontaneous polariton scattering (noise), stimulated scattering term (included in the form of a saturated gain, accounting for scattering from the reservoir) and kinetic energy relaxation that takes the form of an energy-dependent decay term [1]:

$$i\hbar \frac{\partial \Psi}{\partial t} = -(1 - i\Lambda) \frac{\hbar^2}{2m} \Delta \Psi + \alpha |\Psi|^2 \Psi - \frac{i\hbar}{2\tau} \Psi + \left(U(\mathbf{r}) + U_R(n) \exp\left(-\frac{(\mathbf{r} - \mathbf{r}_0)^2}{\sigma^2}\right) \right) \Psi + i\gamma(n) \exp\left(-\frac{(\mathbf{r} - \mathbf{r}_0)^2}{\sigma^2}\right) \Psi + \xi. \quad (1)$$

Here m is the polariton mass, $\Lambda = 3 \times 10^{-3}$ is the kinetic energy relaxation term, $\alpha = 3E_b a_b^2$ is the polariton-polariton interaction constant ($E_b = 10$ meV is the exciton binding energy and $a_b = 10$ nm is the exciton Bohr radius), $U(\mathbf{r})$ is the honeycomb lattice potential (height 20 meV), containing an imaginary part accounting for the shorter lifetime induced by the evanescent part of the modes outside of the pillars. $U(\mathbf{r})$ eventually gives rise to the honeycomb dispersion, including the S and P bands. $U_R(n)$ is the potential induced by the reservoir, which we take to be equal to 1 meV for the considered injected polariton density n . The reservoir has a Gaussian shape with a width of 45 μm given by the size of the excitation spot. τ is the polariton lifetime (30 ps), $\gamma(n)$ is the saturated stimulated scattering rate from the reservoir to the condensate, and ξ is the Gaussian noise term with amplitude $10^{-3} \hbar/2\tau$.

For this set of parameters the simulations reproduce condensation at the Γ point on the top of the π^* band, as in the experiment. The condensation mechanism in that negative mass state can be understood as follows. First, the reservoir of excitons created by the nonresonant pump creates a repulsive potential for polaritons, which

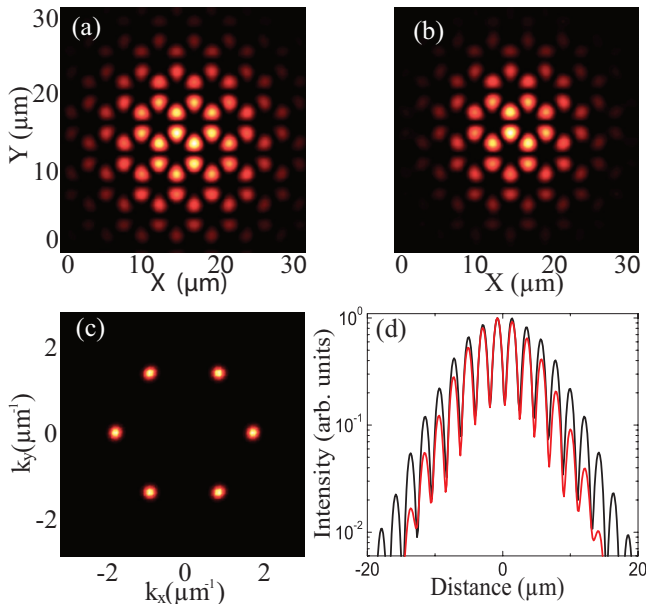


FIG. 2. Spatial image of the condensate constructed from the simulation of the modified 2D Gross-Pitaevskii equation (Eq.1) with (a) negligible interactions $\alpha |\Psi|^2 \ll U_R(n)$ and (b) significant interactions $\alpha |\Psi|^2 \sim U_R(n)$. (c) Fourier transform of the simulated emission corresponding to (a). (d) Spatial transverse profile passing through the center of the excitation spot extracted from (a) (black) and (b) (red).

pushes away particles created by spontaneous scattering, preventing the formation of the condensate in the states with positive mass. However, the states with negative mass are on the contrary trapped in this potential, and serve as a seed for stimulated scattering. A second reason for the condensation of polaritons on top of the π^* band is that the lifetime of anti-symmetric states is in general longer than that of the symmetric one [2]. This is due to the fact that the evanescent fraction of the mode outside the pillars is reduced for these modes due to the presence of the zeroes of the wavefunction at all junctions between the pillars, where there is a larger density of non-radiative centers that contribute to the lifetime reduction. This aspect favors the Γ point of the π^* band with respect to (for example) the Γ points of the non-flat P bands, which might also have negative mass, or with respect to the flat band, which possess much shorter lifetimes due to the location of the wavefunction lobes on the junctions between the pillars (see Fig. 4(b) of the main text).

Figure 2(a) shows the simulated emission from the condensate in the real space and Fig. 2(c) in the reciprocal space, in the absence of polariton-polariton interactions ($\alpha |\Psi|^2 \ll \frac{\hbar}{2\tau}, U_R(n)$). The simulation is in quantitative agreement with the experimental observations (Figs. 3(b) and (a), respectively), including the absence of emission from the Γ point in the first Brillouin zone due to interference effects. When varying the position of the pump spot with respect to the center of the lattice, a very similar

spatial and momentum space patterns are obtained.

The spatial extension of the condensate coincides with that of the excitation spot that populates the reservoir. When interactions in the condensate become non-negligible compared to the interactions induced by the reservoir ($\alpha |\Psi|^2 \sim U_R(n)$) we expect the state to evolve into a gap soliton bound to the reservoir, as a consequence of the same mechanisms that have allowed its observation in a 1D periodic lattice for polaritons [3]. The increase of the polariton-polariton interaction term $\alpha |\Psi|^2$ in the simulation leads to the shrinking of the spatial extension of the emission (see Fig. 2(b)). Even the smallest interactions within the condensate bring its energy up, further into the gap. The modification of the simulated transverse profile of the condensate corresponding to Fig. 2(a, b) is shown in Fig. 2(d). Limitation in the highest available excitation density in the experiment prevents us from seeing the expected modification in the spatial profile when the condensate evolves into a gap soliton.

P BANDS: 2D SCHRÖDINGER EQUATION SIMULATION

In order to confirm the phenomenological model used to describe the results reported in Fig. 4, in which we assume that the tunnelling probability is energy dependent, we have performed a 2D Schrödinger equation simulation for polaritons in the low density limit. Since the S and P bands are located close to the bottom of the lower polariton branch, we use the effective mass approximation:

$$i\hbar\partial_t\Psi = -\frac{\hbar^2}{2m}\Delta\Psi + \left(U - \frac{i\hbar}{2\tau}\right)\Psi + P_0 e^{-\frac{(t-t_0)^2}{\tau_0^2}} e^{-\frac{(x-r_0)^2}{\sigma^2}} e^{-i\omega t}. \quad (2)$$

Here m is the polariton mass, $\tau = 30$ ps is the polariton lifetime, and U is the external potential describing the etched honeycomb lattice. In our simulation we use a rectangular sample made out of coupled micropillars of round geometry and same dimension as in the experiment, arranged in a lattice with 16 by 16 unit cells. The height of the polariton confining potential in the micropillars was taken 20 meV. The last term of the equation simulates a pulsed probe that will excite the different eigenstates of the Schrödinger equation, thus allowing their visualization. P_0 is the amplitude of the probe, arriving at the sample at t_0 , $\tau_0 = 0.2$ ps is the pulse duration, $\sigma = 0.7 \mu\text{m}$ the spot size. Using a short pulse and a small spot allows exciting several bands of the dispersion at the same time. \mathbf{r}_0 is the pump location (center of the sample, which does not correspond to the center of a particular pillar) and ω is the pump central frequency, centered 4 meV above the bottom of the lower polariton

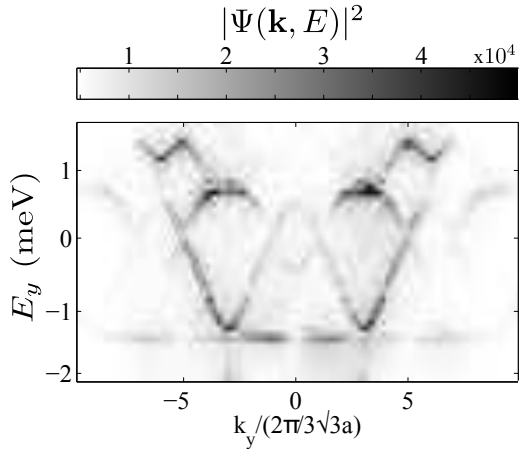


FIG. 3. Simulation of $|\Psi(\mathbf{k}, E)|^2$ along the same momentum space direction as Fig. 4(a) in the main text, based on the solution of Eq. 2.

branch to mainly excite the P band multiplet. Let us note that the probe pulse excites different parts of the dispersion with different efficiency, depending on their symmetry.

The Schrödinger equation is then integrated over time for 100 ps with a spatial grid 512×512 (the size of the grid is $80 \times 80 \mu\text{m}$) using a NVIDIA graphic card. The solution

of the equation $\Psi(\mathbf{r}, t)$ is then Fourier-transformed over time and space to obtain the dispersion $|\Psi(\mathbf{k}, E)|^2$. The result is shown in Fig. 3 along the same momentum-space direction as in Fig. 4(a) of the main text. The simulation is in excellent quantitative agreement with the experimental observation: the lowest P band is indeed flat, while the upper band is dispersive. The full 2D model reproduces this behavior correctly, because it automatically takes into account the exponential increase with energy of the tunneling rate of the P states of the individual pillars, as explained in the main text and illustrated by the tight-binding model calculations.

* Now at IM2NP UMR CNRS 7334 Aix-Marseille Université

- [1] E. Wertz, A. Amo, D. D. Solnyshkov, L. Ferrier, T. C. H. Liew, D. Sanvitto, P. Senellart, I. Sagnes, A. Lemaître, A. V. Kavokin, G. Malpuech, and J. Bloch, *Physical Review Letters* **109**, 216404 (2012).
- [2] I. L. Aleiner, B. L. Altshuler, and Y. G. Rubo, *Physical Review B* **85**, 121301 (2012).
- [3] D. Tanese, H. Flayac, D. Solnyshkov, A. Amo, A. Lemaître, E. Galopin, R. Braive, P. Senellart, I. Sagnes, G. Malpuech, and J. Bloch, *Nature Communications* **4**, 1749 (2013).